Chapter 5

Spectroscopic Investigation of Tetramethyl Rhodamine Quenching by N-methyl Imidazole, N-methyl Pyrrole, and β-alanine Linked Polyamides

The work described in this chapter was completed in collaboration with my good friend Alexander R. Dunn of Professor Harry Gray's group. Jay R. Winkler provided the algorithm for data fitting.

Abstract

The fluorescence from tetramethyl rhodamine in hairpin polyamide tetramethyl rhodamine (TMR) conjugates is quenched in solution. TMR fluoresces brightly upon polyamide binding match DNA. Similar behavior is not observed in the presence of mismatch DNA; the hairpin polyamide-fluorophore conjugates therefore provide a small-molecule fluorescent means for detecting chosen DNA sequences in homogenous samples. In Chapter 4, we reported the DNA recognition behavior of hairpin polyamide-fluorophore conjugates as examined by steady-state fluorescence. Here we provide information concerning the mechanism of TMR quenching in the TMR-polyamide conjugates. Evidence from time-resolved fluorescence and steady-state fluorescence and absorption spectroscopy indicates that an intramolecular ground state complex forms between the fluorophore and the polyamide. Ground-state contact between the fluorophore and polyamide likely facilitates quenching of the TMR excited state by electron transfer from the N-methyl pyrrole moieties in the polyamide.

Introduction

As discussed in the introduction, hairpin polyamides are synthetic ligands that recognize the minor groove of double stranded DNA with high affinity and sequence specificity.[1] As reported in Chapter 4, the fluorescence of tetramethyl rhodamine (TMR) is efficiently quenched when covalently attached to the ring nitrogen of a pyrrole residue within a hairpin polyamide.[2] Remarkably, the TMR fluorescence is restored when the

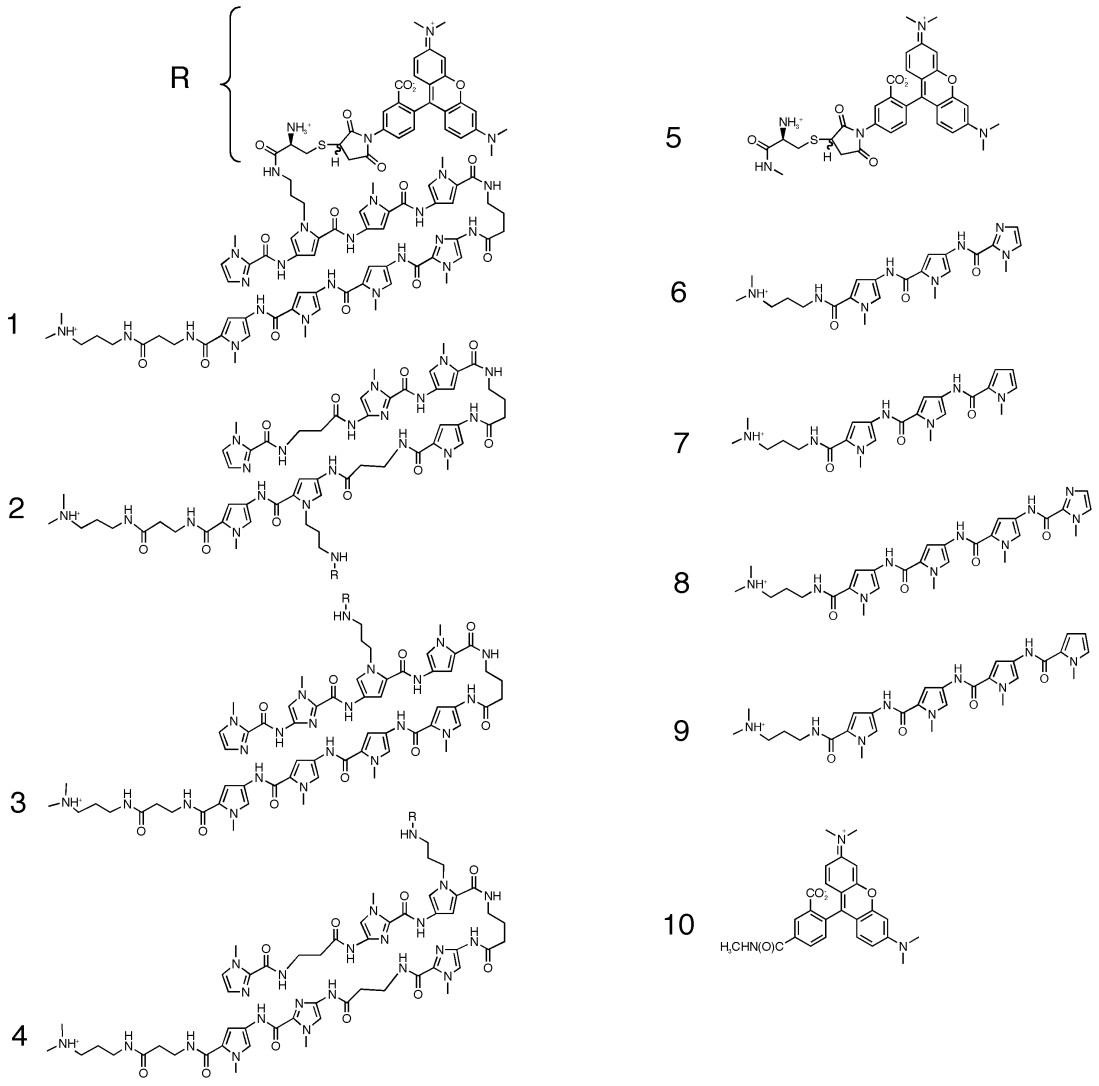

Figure 5.1 Chemical structures of compounds studied. **R** indicates the chromophore shown in **1** and abbreviated in chemical structures **2** – **4**.

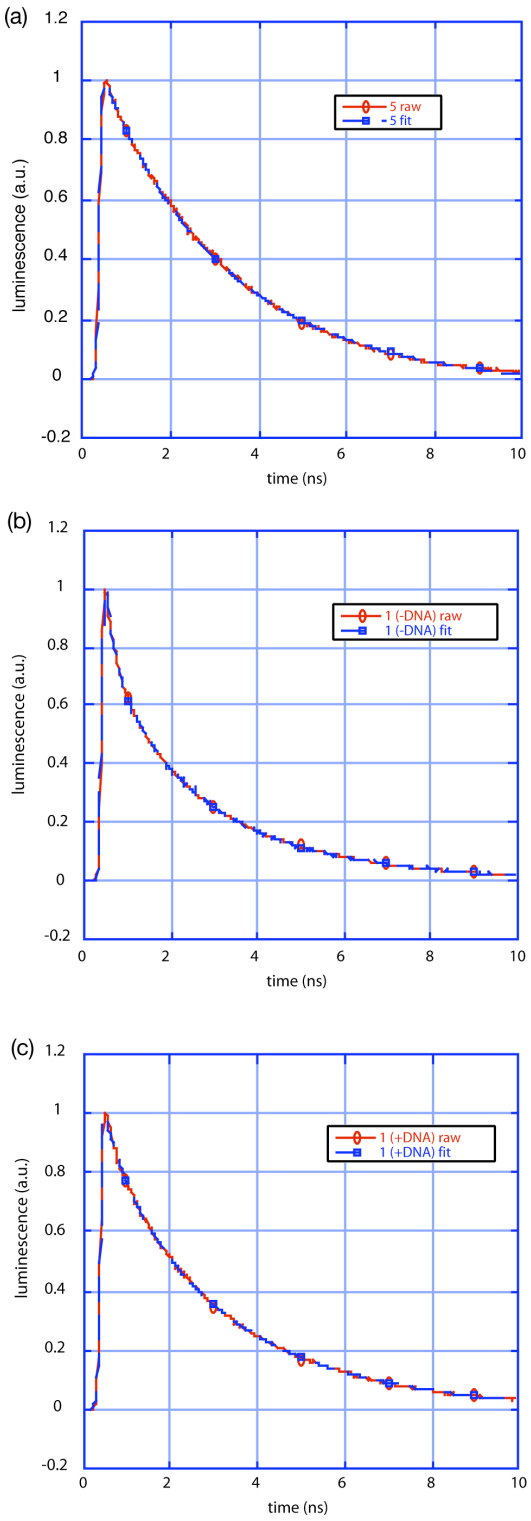

Figure 5.2 Observed luminescence decay for control **5** (a), 3 μM **1** in the absence (b) and presence (c) of 6 μM match DNA. The time window is 10 ns.

polyamide-fluorophore conjugate binds to double stranded DNA. The fluorophore remains quenched if the DNA does not contain the polyamide's match recognition site, indicating that the restoration of fluorescence results from sequence specific binding in the minor groove.

In order to better understand this remarkable sequence specific luminescence enhancement, we studied the photophysics of the TMR-polyamide conjugates (renumbered from Chapter 4) **1** – **4** and control **5** using both steady-state and time-resolved luminescence measurements (Figure 5.1). In addition, the intermolecular interactions of the TMR fluorophore **10** with the polyamide fragments **6** – **9** were examined using steady-state absorption and fluorescence spectroscopies. Our results indicate

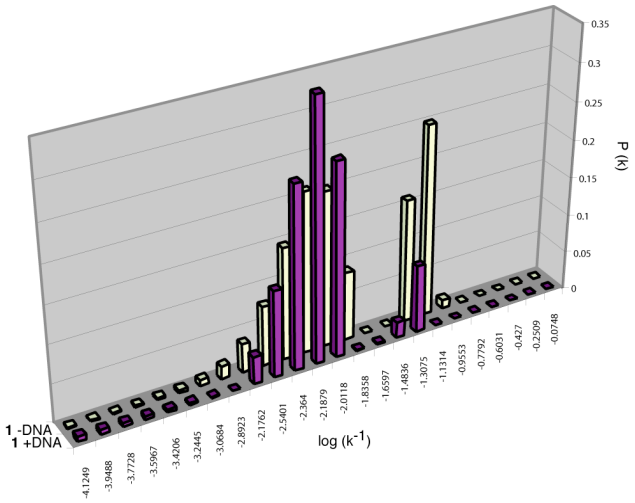

Figure 5.3 Maximum entropy fitting calculated rate constant distribution for **1** in absence (-DNA) and presence (+DNA) of match DNA.

that TMR quenching in conjugates **1** - **4** is mediated by intramolecular hydrophobic interactions between the TMR and polyamide. We suggest electron transfer from the polyamide, most likely a N-methyl pyrrole moiety, to the singlet excited state of the fluorophore as a plausible quenching mechanism.

Experimental procedures

All samples used in time-resolved studies were prepared in phosphate buffered Milli-Q water. Steady-state spectra were collected in 1X tris-EDTA buffered Milli-Q water. Time resolved fluorescence spectra were recorded with a Hamamatsu C5680 streak camera using the 3rd harmonic (290 nm) of a regeneratively amplified femtosecond Ti:Sapphire laser (Spectra-Physics) for the excitation pulse.[3] Steady-state fluorescence spectra were collected on a Hitachi F-2500 fluorometer with samples excited at 545 nm. Absorption spectra were collected on a HP1045 absorption spectrometer. All samples were purged with argon for time-resolved spectroscopy. Quantum yield measurements were made relative to sulforhodamine 101 as published.[4] DNA was synthesized by Genbase, Inc. (San Diego, CA) and used and stored as previously described.[2] Cuvettes were from Starna. Compounds **1 – 5** were synthesized as previously reported.[2,5] 5-

A

-DNA	$\Sigma P(k_{fast})$	$\Sigma P(k_{slow})$	$\frac{\Sigma P(k_{fast})}{[\Sigma P(k_{fast}) + \Sigma P(k_{slow})]}$	τ_{fast} (ns) (mean)	τ_{slow} (ns) (mean)
1	0.38	0.85	0.31	1.3	4
2	0.28	0.89	0.24	"	"
3	0.42	0.76	0.34	"	"
4	0.32	0.73	0.27	"	"
5	-	1.13	-	-	"

B

+DNA	$\Sigma P(k_{fast})$	$\Sigma P(k_{slow})$	$\frac{\Sigma P(k_{fast})}{[\Sigma P(k_{fast}) + \Sigma P(k_{slow})]}$	τ_{fast} (ns) (mean)	τ_{slow} (ns) (mean)
1	0.11	1.02	0.1	1.3	4
2	0.11	1.05	0.09	"	"
3	0.18	0.97	0.16	"	"
4	0.1	1.08	0.09	"	"

Table 5.1 P(k) distribution for **1 – 5** in the absence of DNA (A) and for **1 – 4** when bound to match DNA (B). Lifetimes for the 4- and 1.3-ns luminescence decay are shown in the right of the table.

carboxy- tetramethyl rhodamine, succinimidyl ester, was reacted with methylamine to provide **10** after preparatory HPLC purification. Compounds **6 – 9** were prepared using oxime resin and also purified by preparatory HPLC. All compounds were verified by MALDI/TOF mass spectrometry and analytical HPLC. For **6** (monoisotopic) [M + H] 456.67 (455.25 calc'd for $C_{22}H_{31}N_8O_3$); **7** (monoisotopic) [M + H] 455.38 (454.26 calc'd for $C_{23}H_{32}N_7O_3$); **8** (monoisotopic) [M + H] 578.85 (577.30 calc'd for $C_{28}H_{37}N_{10}O_4$); **9** (monoisotopic) [M + H] 577.20 (576.30 calc'd for $C_{29}H_{38}N_9O_4$); **10** (monoisotopic) [M + H] 444.54 (443.18 calc'd for $C_{26}H_{25}N_3O_4$).

The streak camera response function was determined using scattered light from buffered water. The luminescence decay kinetics were determined for compounds **1 – 4** in the presence and absence of match DNA. The luminescence decay kinetics for **5** were collected in phosphate buffered Milli-Q water. The fitting of luminescence decay

kinetics was performed by maximum entropy fitting (ME) as previously described.[3] All data presented in this chapter are the average of at least three determinations.

Results

Dynamic and steady-state spectroscopy on 1 – 5

We observe monophasic luminescence decay for **5** with a lifetime of 4 ns (Figure 5.2a) Conjugates **1** – **4** show biphasic luminescence decays in the absence of match DNA, and ~ 90% monophasic decay (Figure 5.2b, 5.2c) with lifetimes identical to that of **5** upon binding match DNA. In Figure 5.3, we show the rate constant (k) distribution for **1** in the presence and absence of match DNA. The rates cluster with mean lifetimes of 4- and 1.3-ns. Rate constant weightings [P(k)] for conjugates **1** – **4** in the presence and absence of DNA, and the monophasic decay from control **5**, are shown in Table 5.1. Binding of the fluorescent probe molecules to the target DNA sequences results in a decrease in the weighting of the fast phase of

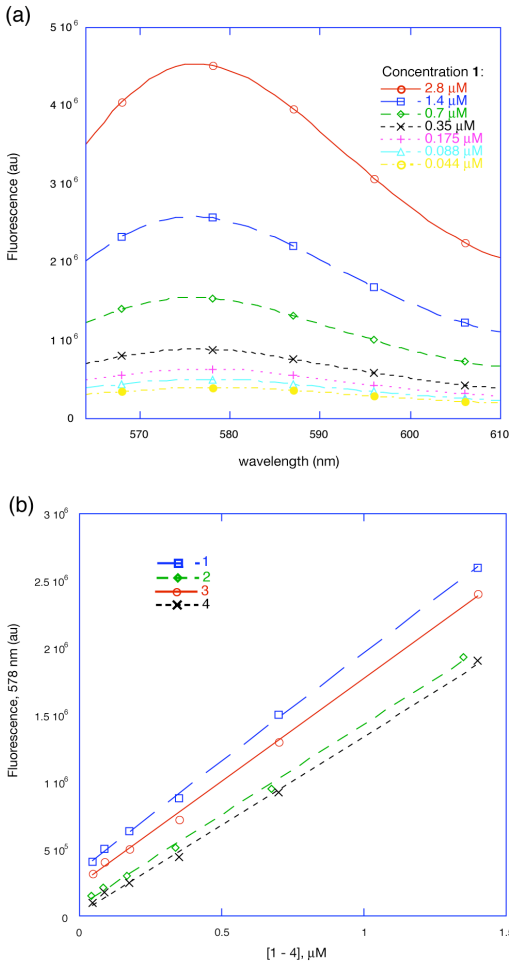

Figure 5.4 (a) Dilution of **1** from 1.4 μM to 44 nM. (b) Fit of linear decrease in fluorescence for compounds **1** – **4** over similar concentration range to that shown for **1** above.

luminescence decay from ~30% to ~10%.

The quantum yields of the conjugates, relative to sulforhodamine 101, are: **1**, 0.009; **2**, 0.04; **3**, 0.01; **4,** 0.03 in the absence of DNA. Upon binding match DNA, the quantum yields increase dramatically: **1**, 0.52; **2**, 0.50; **3**, 0.57; **4**, 0.38**.** The quantum yield for **5**, the TMR control compound, is 0.71. The discrepancy between the modest changes in the lifetime distributions and the significant fluorescence increases upon binding of the polyamide in the minor groove of DNA suggests the presence of a third very rapid, unresolved decay pathway. The observed quantum yield (Φ) can be described using three decay rates ($k_{1\text{-}3}$) and weightings ($c_{1\text{-}3}$): $\Phi = c_1k_r/k_1 + c_2k_r/k_2 + c_3k_r/k_3$. The rates k_1 and k_2 correspond to the observed 4- and 1.3-ns lifetimes, while k_3 is unresolved. k_r is the radiative rate constant determined from the observed monophasic luminescence decay of **5**. From the observed quantum yields and known decay rates, we estimate that k_3 is greater than 5 x 10^9 s^{-1}, corresponding to a

[1]	$\Sigma P(k_{fast})$	$\Sigma P(k_{slow})$	$\frac{\Sigma P(k_{fast})}{[\Sigma P(k_{fast}) + \Sigma P(k_{slow})]}$
0.5 μM	0.38	0.84	0.31
1 μM	0.33	0.85	0.28
5 μM	0.33	0.85	0.28
[2]			
0.5 μM	0.25	0.89	0.22
1 μM	0.22	0.94	0.19
5 μM	0.28	0.89	0.24
[3]			
0.5 μM	0.36	0.81	0.31
1 μM	0.46	0.79	0.37
5 μM	0.42	0.81	0.35
[4]			
0.5 μM	0.33	0.83	0.28
1 μM	0.29	0.88	0.25
5 μM	0.32	0.87	0.27

Table 5.2 Dilution of **1** – **4** over 1 order of magnitude induces no change in P(k) as expected for static quenching. This data says nothing about whether the quenching mechanism is intramolecular or intermolecular.

lifetime of less than 200 ps. The P(k) weighting of this pathway, which likely corresponds to nonradiative depopulation of the excited state, is ~ 93% in the absence of DNA. The weighting of k_3 decreases to ~ 26% when the polyamide DNA recognition domain is bound in the minor groove while the population corresponding to k_1 (= k_r for **5**) becomes ~ 67% of the P(k).

Dilution of solutions (~3 μM to ~40 nM) of **1** – **4** in the absence of DNA resulted in a decrease in the fluorescence intensity at 578 nm linearly dependent on the concentration of conjugate (Figure 5.4). These data indicate that the observed quenching is unlikely the result of intermolecular (and hence concentration dependent) fluorophore aggregation. Instead, the fluorescence decrease linear in concentration is consistent with an intramolecular quenching mechanism. Additionally, lifetime measurements on solutions of **1** – **4** diluted over an order of magnitude from 5 μM to 500 nM resulted in invariant lifetime distributions. This observed concentration independence for lifetime distribution is indicative of a static quenching mechanism consistent with emission observed only from unperturbed fluorophores with distributions that should not change upon

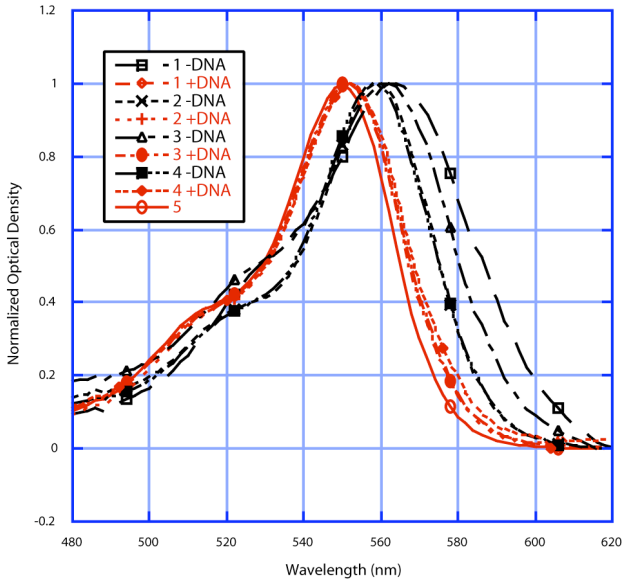

Figure 5.5 Steady-state absorption spectra of **1** – **4** in the absence (black lines) and presence (red lines) of 1 equivalent match DNA. Absorption of control **5** is also shown for comparison purposes.

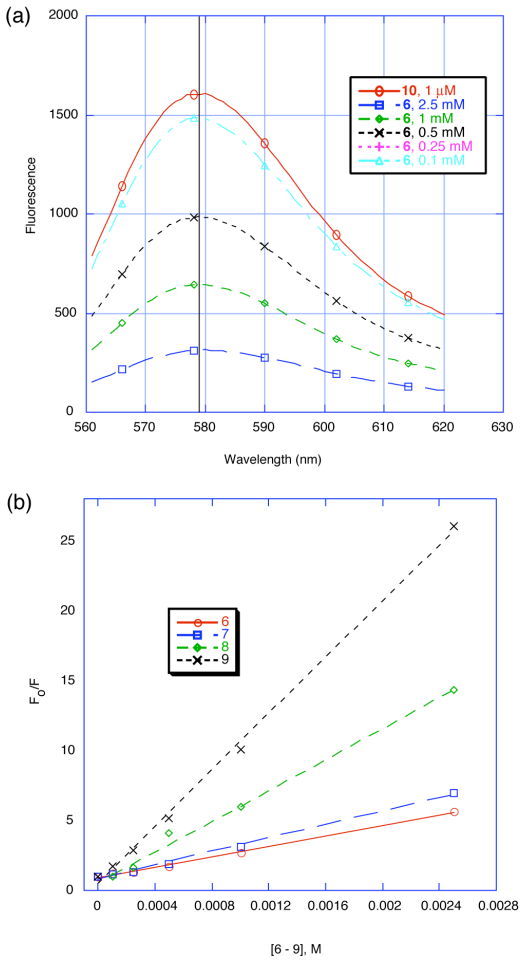

Figure 5.6 (a) Emission spectrum of 1 μM **10** in the presence of increasing concentration of quencher **6**. Note the invariance in emission maximum as shown by black line. (b) Fit of ratio of fluorescence in absence (F_o) and presence (F) of increasing concentration of polyamide quencher **6** against polyamide concentration.

dilution (Table 5.2).

The steady-state absorption spectrum of a chromophore may be perturbed in the presence of molecules that interact with the chromophore in the ground state.[6-11] We observe pronounced bathochromic shifts in the absorption spectra of **1** – **4** as compared to **5**, a phenomenon noted for ground state interactions involving the related xanthene fluorophore fluorescein.[12] There is a marked blue-shift upon binding of the polyamide to match DNA (Figure 5.5). Note that this hypsochromic shift places the TMR absorption of **1** - **4** almost exactly over the absorption spectrum of control **5**. This behavior suggests that the ground state interaction between the TMR and the polyamide is disrupted upon DNA binding, presumably by sequestration of the polyamide in the minor groove. This behavior suggests that static quenching is the mechanism for fluorescence quenching in the absence of DNA.

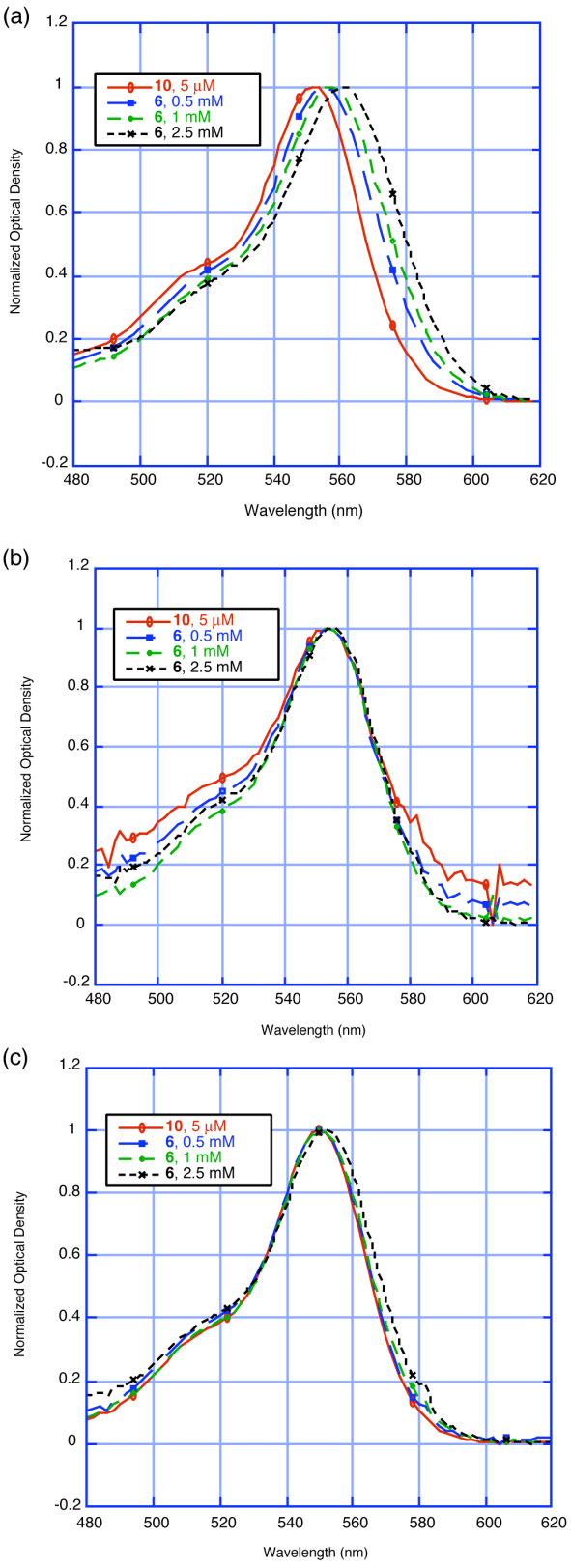

Figure 5.7 (a) Steady-state absorption spectra of 5 μM **10** with increasing concentrations of **6**. (b) Steady state absorption spectra of **10** in 50% (v/v) DMSO:H_2O in presence of identical concentration gradient used in panel (a). (c) Steady state absorption spectra of **10** in 50% (v/v) methanol:H_2O in presence of identical concentration gradient used in panel (a). Note that organic solvent abrogates the red shift observed in aqueous solution.

Steady-state absorption and fluorescence spectroscopy on 6 – 10.

A 1 μM solution of **10** was excited at 545 nm in the presence of 0.1, 0.25, 0.5, 1, and 2.5 mM **6** – **9**. We observe a linear decrease in fluorescence as the concentration of any given polyamide fragment **6** – **9** is increased (Figure 5.6a, 5.6b). Fitting the ratio of fluorescence from **10** in the absence of polyamide (F_o) and presence of polyamide (F) to the Stern-Volmer equation for static quenching ($F_o/F=1 + K_q[Q]$) allows us

to ascertain physically reasonable quenching association constant K_q for the interaction of **6 – 9** with **10** (Table 5.3). In contrast, fitting the data to a dynamic quenching model (F_o=1 + $k_q\tau_o$[Q]), where τ_o (~ 4 ns) is the luminescence lifetime of **10** and k_q is the bimolecular quenching rate constant, results in calculated values of k_q that are larger than

	K_q x 10^{-3} (M^{-1})	Em_{max}[a] (nm)	Abs_{max}[b] (nm)	ΔAbs[c]
1	1.88	578-580	**562**, 554, 552	10
2	2.41	"	**562**, 554, 552	10
3	6.48	"	**566**, 556, 554	12
4	10.11	"	**568**, 556, 556	14
5	n/a	"	**552**, 554, 552	-

All values are the average of three determinations. [a]Note invariance in emission maximum. [b]First column indicates maximum observed bathochromic shift in aqueous solution for concentrations described, second column is absorption values in 50% (v/v) DMSO:water, third column is absorption values in 50% (v/v) methanol:water. [c]These are the maximum shifts in absorption values.

Table 5.3 Values of quenching association constant, emission maximum, and absorption values for the association of **6 – 9** with a 1 μM concentration of **10**.

the maximum rates allowed by diffusion ($k_q > 10^{10}$ $M^{-1}s^{-1}$).[13] We also note invariance in the fluorescence emission maximum of the **10** under increasing concentrations of **6 – 9**, a result consistent with a non-emissive TMR•polyamide complex.[8,14-17]

The steady-state absorption spectra of 5 μM of **10** with increasing concentrations of **6 – 9** demonstrate a large concentration dependent bathochromic shift (Figure 5.7, Table 5.3). We postulate once again that this spectral shift is the product of a ground state interaction between **10** and the polyamide. In contrast, no change in the absorption spectrum of **10** is observed when solutions are made using 50% (v/v) dimethyl sulfoxide

(DMSO) or methanol (MeOH) as added organic co-solvent. Presumably, the organic co-solvents disfavor hydrophobic interactions between **10** and the polyamides, thus preventing association. This observation is in accord with our previous observation (Figure 4.9) whereby increasing DMSO co-solvent induces an increase in quantum yield for conjugates **2** – **7** (Figure 4.3, Figure 4.6) presumably by a similar mechanism of disfavoring the polyamide-fluorophore hydrophobic collapse that leads to quenching.

Conclusions

Interest in non-denaturing means for the sequence specific fluorescence detection of DNA has prompted us to undertake photophysical studies to further our understanding of how the fluorophore tetramethyl rhodamine is quenched when covalently attached to a sequence specific DNA binding hairpin polyamide. We hypothesize that an

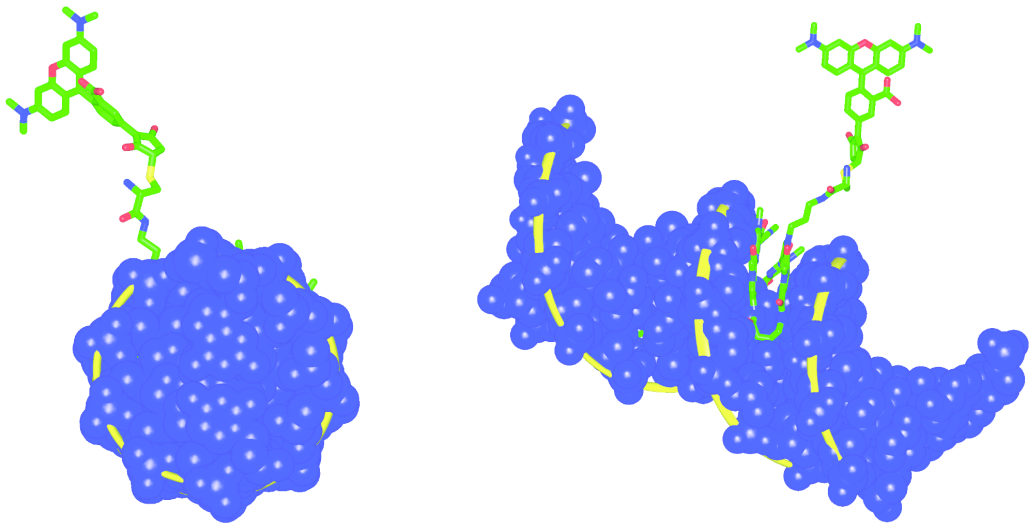

Figure 5.8. Molecular model of hairpin polyamide-TMR conjugate docked in the minor groove (hydrogens not shown). Upon addition of DNA containing the polyamide-TMR conjugate's match recognition site, the polyamide binds in the minor groove while the fluorophore remains in solution and fluorescence is restored. Note that binding completely precludes fluorophore access to the polyamide.

intramolecular complex forms in the ground state between the fluorophore and the hairpin polyamide to which it is attached. Upon DNA binding, the polyamide is inaccessible to the fluorophore (Figure 4.12, Figure 5.8). Upon excitation, > 90% of the molecules are rapidly quenched (< 200 ps). Much smaller populations undergo luminescent decays with lifetimes of 4- and 1.3-ns, possibly indicating conformational or protonation heterogeneity within the conjugate sample.[18,23]

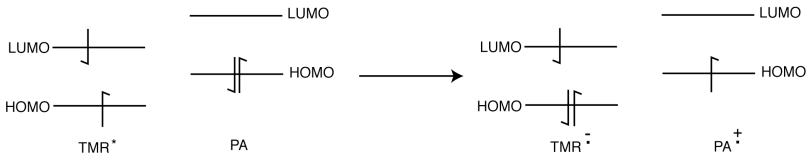

Figure 5.9 Excited state electronic model for reductive quenching of singlet excited state of tetramethyl rhodamine. After generating the fluorophore excited state (left panel), there is rapid electron transfer from the polyamide to the fluorophore. This charge-separated species rapidly decays to the ground state and releases heat.

The lack of spectral overlap between the TMR emission and polyamide absorption spectra precludes a Förster energy transfer quenching mechanism. In contrast, the known photophysical properties of rhodamine fluorophores ($E_{red}^{o(*)/-}$ = 1.4 V vs. NHE),[10,19,24] and electrochemistry of N-methyl pyrrole derivatives (E_{ox}^{o} = 1.0 V vs. AgCl)[20] makes an electron transfer quenching mechanism quite plausible (Figure 5.9).[21,22] Reductive quenching of xanthene fluorophores similar to TMR has been observed for nucleobase-excited state fluorophore interactions,[10,19] and extremely short lifetimes as proposed here have been observed for electron transfer quenching of fluorescein complexed with anticalin.[11]

References

1. Dervan, P. B. (2001) *Bioorg. & Med. Chem.* **9**, 2215-2235.

2. Rucker, V. C., Foister, S., Melander, C. & Dervan, P. B. (2002) *J. Am. Chem. Soc.* **125**, 1195-1202.

3. Lyubovitsky, J. G., Gray, H. B. & Winkler, J. R. (2002) *J. Am. Chem. Soc.* **124**, 5481-5485.

4. Karstens, T. & Kobs, K. (1980) *J. Phys. Chem.* **84**, 1871-1872.

5. Belitsky, J. M., Nguyen, D. H., Wurtz, N. R. and Dervan, P. B. (2002) *Bioorg. & Med. Chem.* **10**, 2767-2774.

6. Johansson, M. K., Fidder, H., Dick, D., Cook, R. M. (2002) *J. Am. Chem. Soc.* **124**, 6950-6956.

7. Armitage, B., Retterer, J., O'Brien, D. F. (1993) *J. Am. Chem. Soc.* **115**, 10786-10790.

8. Lakowicz, J. R. (1999) *Principles of Fluorescence Spectroscopy* (Kluwer Academic/Plenum Publishers, New York), 2nd Ed.

9. Schenk, G. H. (1973) *Absorption of Light and Ultraviolet Radiation: Fluorescence and Phosphorescence Emission* (Allyn and Bacon, Inc., Boston)

10. Seidel, C. A. M., Schulz, A., Sauer, M. H. M. (1996) *J. Phys. Chem.* **100**, 5541-5553.

11. Götz, M., Hess, S. Beste, G., Skerra, A., Michel-Beyerle, M.E. (2002). *Biochem.* **41**, 4156-4164.

12. Voss Jr., E. W., Croney, J. C., Jameson, D. M. (2002) *J. Prot. Chem.* **21**, 231-241.

13. Tinoco Jr., I., Sauer, K., Wang, J. C., Puglisi, J. D. (2002) *Physical Chemistry: Principles and Applications in Biological Sciences* (Prentice Hall, New Jersey) p. 353.

14. Nemzek, T. L. & Ware, W. R. (1975) *J. Chem. Phys.* **62**, 477-489.

15. Eftink, M. R. & Ghiron, C. A. (1976) *J. Phys. Chem.* **80**, 486-493.

16. Rabinowitch, E. & Epstein, L. F. (1941) *J. Am. Chem. Soc.* **63**, 69-78.

17. Kubota, Y., Motoda, Y., Shigemune, Y., Fujisaki, Y. (1979) *Photochem. &*

Photobiol. **29**, 1099-1106.

18. Edman, L., Mets, Ü, Rigler, R. (1996) *Proc. Nat. Acad. Sci.* USA **93**, 6710-6715.

19. Torimura, M., Kurata, S., Yamadda, K., Yokomaku, T., Kamagata, Y., Kanagawa, T., Kurane, R. (2001) *Analytical Sci.* **17**, 155-160.

20. Kim, O.-K., Lee, Y. S. (1990) *Mol. Cryst. Liq. Cryst.* **190**, 9-18.

21. Lowry, T. H. & Richardson, K. S. *Mechanism and Theory in Organic Chemistry* (Harper & Row, New York), 3rd Ed., p. 232.

22. Using the Rehm-Weller equation, [$\Delta G^{o*}=E_{1/2}^{o}(PA/PA^{+})- E_{1/2}^{o}(F^{-}/F)^{(*)}-E_{00}$], it is possible to estimate the free-energy change associated with an photo-induced electron transfer event. E_{00} is the energy of the zero-zero excitation from the ground state to the singlet excited state.

23. Wennmalm, S., Edman, L., Rigler, R. (1997) *Proc. Natl. Acad. Sci. USA* **94**, 10641-10646.

24. Yasui, S., Tsujimoto, M., Itoh, K., Ohno, A. (2000) *J. Org. Chem.* **65**, 4715-4720.